Alginate-εPLL core-shell hydrogel beads as a tool for an effective, stable and scalable microbial encapsulation

Alba Amaro-Cruz[1], Miguel García-Román[1], Ignacio Moya-Ramírez[*1]

[1]Chemical Engineering Department, Faculty of Sciences, University of Granada. Campus Fuentenueva, 18071, Granada, Spain.

[*]Corresponding author: ignaciomr@ugr.es

Abstract: Synthetic microbial consortia offer significant potential for biotechnological applications. However, achieving stable and reproducible co-cultures is challenging due to competitive dynamics and unbalanced growth rates among species. Here, we present an effective method for microbial encapsulation based on alginate-based core-shell hydrogel beads coated with ε-poly-L-lysine (εPLL-HB). This method ensures complete microbial containment while allowing for consistent growth inside the beads of several microbial species with a wide variability in their features. Compared to chitosan and α-poly-L-lysine, two of the most used coating agents for this kind of encapsulation, εPLL demonstrated superior performance in avoiding cellular escape across diverse culture conditions and for all the microbial strains tested, while allowing their proliferation inside the capsule. εPLL-HB enabled the construction of spatially organized co-cultures, effectively balancing populations between microorganisms with different growth rates. Furthermore, εPLL-HB provided protection against toxic compounds in lignocellulosic-derived media and maintained their encapsulation efficacy and viability after long-term storage at -80°C. The superior microbial containment, structural integrity and chemical resistance of εPLL-HB, combined with their low price and ease of preparation, makes them a versatile tool for engineering synthetic microbial consortia, with broad applicability in biotechnological processes.

1. Introduction

Communities of co-occurring and interacting microorganisms are complex systems ubiquitous in nature. They represent the natural endpoint in most environments where microorganisms have naturally evolved [1,2]. By exploiting the traits emerging from their synergistic interactions, microbial consortia have the potential to challenge the current single strain-based paradigm in microbial biotechnology [3]. Examples of these traits are the enhanced metabolic capabilities due to division of labour, which can result in reduction of cellular burden and higher productivities or wider range of metabolizable carbon sources compared to single-species cultures [4,5]. They also show better stability and resilience to changes in the environment [6]. Natural microbial consortia have been traditionally used for composting and anaerobic digestions [7], while synthetic ones, normally referred as co-cultures, have been developed focusing on diverse applications in biochemical synthesis and environmental remediation for example [8–13].

However, harnessing the full potential of microbial consortia requires effective strategies to manipulate and engineer them [14]. Focussing on the engineering of synthetic microbial consortia, these face a main challenge in maintaining balance among co-cultured species [15]. In liquid microbial co-cultures, differences in the growth and nutrient consumption dynamics between the species and other competitive interactions will normally lead to one species uncontrolledly outgrowing the rest. This lack of populations control dramatically reduces the

number of the microorganisms that can be co-cultured [16]. Besides, addressing this limitation is necessary to obtain stable and reproducible co-cultures, which otherwise will not be suitable for their engineering and scaling-up.

Spatial organization and microbial encapsulation allow a precise control over microbial populations, and therefore, are being used as alternatives to co-cultures suspension [16,17]. Besides population control, microbial encapsulation offers other additional advantages such as mimicking microbial biofilms-based niches or protection against environmental stressors and toxic substances [18].

In this regard, hydrogel-based encapsulation technologies stand out for their biocompatibility, tuneable properties and ease of fabrication. Hydrogels also allow the mass transfer of biomolecules, maintaining the chemical communication with the exterior needed for nutrient uptake or cell signalling for example. Alginate hydrogels excel on all these features, and therefore, have been extensively studied for cell encapsulation [19,20]. However, the physical integrity of alginate hydrogels is highly sensible to chelating agents such as citrate or phosphate, and to cations such as Na2+ or Mg^{2+}, that are commonly present in most of the culture media [21]. Additionally, the growth of the encapsulated microbes or osmotic pressures can cause swelling of the alginate hydrogel [18,21], which could lead to the loss of its structural integrity. For this reason, alginate-based core-shell hydrogels, where alginate beads containing the encapsulated cells are coated with other material that improves the mechanical and chemical resistance of alginate are a common approach used in this field [21–23].

When applied to microbial co-cultures, avoiding cell escape from their confined space is another desired feature in any cell encapsulation approach. Otherwise, the population balance could be compromised by the uncontrolled growth of the released microbes. Despite of the wide range of possible coating materials and techniques described for alginate core-shell microbial encapsulation, few of them address cell leakage in complex environments and scalable conditions. Wang et al. were able to co-culture several bacterial and yeast strains based on chitosan-coated alginate beads, that by a preliminary analysis did not show cell escape [15]. But to our knowledge, and only recently, Jeong et al. reported core-cell alginate capsules, with coating layers composed however exclusively of alginate, and systematically evaluated the conditions where no cell escape could be detected [18].

In the present work we describe a methodology suitable to encapsulate a wide variety of microbial species that ensures both, a total microbial entrapment inside the HB and their growth inside of them and maintained this encapsulation effective over prolonged periods of time in diverse culture media. We have systematically evaluated the performance of several hydrogel beads (HB) built using a layer-by-layer methodology, comparing three positively charged polymers as coating agents. Two of them are frequently used as coating agents to that end: chitosan and poly-α-L-lysine (α-PLL), and we included in our study poly-ε-L-lysine (ε-PLL), which is less common for these applications and turned out being the best performing of them. Our methodology is exclusively based on low price coating agents and does not need specialized equipment. Its simplicity and compatibility with microfluidics and other automated devices makes it easily scalable and therefore expand the tools for the creation of synthetic microbial co-cultures based on alginate core-shell capsules.

2. Materials and methods

2.1. Microbial strains and chemicals

The bacterial and yeast strains used for this work were *Pseudomonas putida* KT2440 and *Kluyveromyces marxianus* DSM 70792 purchased from the German collection of microorganisms and cell cultures (DSMZ, Germany), *Bacillus subtilis* B5 isolated from oil-rich environments which belongs to our strains collection and *Yarrowia lipolytica* CBS 7504 (W29) purchased from the Westerdijk fungal biodiversity institute (the Netherlands).

Stock cultures of microbial strains were maintained at -80 ºC in LB (bacterial strains) or GPY (yeast strains) supplemented with 25 % (v/v) glycerol. Strains were streaked on LB or GPY agar plates and incubated at 30 ºC for 24 h to obtain isolated colonies.

Natamycin, kanamycin, citric acid, 2-[4-(2-hydroxyethyl)-1-piperazinyl]-ethanesulfonic acid (HEPES), EDTA, alginic acid sodium salt from brown algae (71238), low MW chitosan (448869), poly-α-L-lysine hydrochloride (αPLL) (P2658) (MW 15000–30000 Da), M9 minimal salts and other inorganic reagents were supplied by MERCK (Germany). Poly-ε-L-lysine HCl (εPLL) (MW 3500-4500 Da) was purchased from Biosynth (UK). LB and LB-agar media were obtained from VWR (USA). Yeast extract, peptone, D(+)-glucose and agar powder were supplied by Sharlab (Spain).

2.2. Culture media and buffers

The media used in this work were GPY, minimal medium (M9), and M9-coffee (M9c). GPY consisted of 40 g D(+)-glucose, 5 g peptone and 5 g yeast extract for 1L of solution. When necessary, 15 g/L agar powder was added to prepare GPY-agar plates. M9 was prepared with 33.7 mM Na_2HPO_4, 22.0 mM KH_2PO_4, 8.55 mM NaCl and 9.35 mM NH_4Cl (M9 minimal salts), autoclaved and supplemented with 0.4% D(+)-glucose (w/v), 1 mM $MgSO_4$, 0.3 mM $CaCl_2$, 13.4 mM EDTA, and 3.1 mM $FeCl_3$ from filter-sterilized stock solutions. M9c composition was 50 % (v/v) minimal medium M9 without D(+)-glucose and 50 % (v/v) autoclaved spent coffee grounds hydrolysate.

The buffers used included KRH, phosphate-buffered solution (PBS buffer), and disruption buffer. KRH buffer was prepared with 20 mM HEPES, 135 mM NaCl, 5 mM KCl, 0.4 mM K_2HPO_4, adjusted to pH 7.4 by addition of NaOH, autoclaved, and supplemented with 1 mM $MgSO_4$, and 1 mM $CaCl_2$. PBS buffer consisted of 137 mM NaCl, 2.7 mM KCl, 10 mM Na_2HPO_4, 1.8 mM KH_2PO_4 adjusted to pH 7.4 by addition of NaOH and autoclaved. Disruption buffer was prepared with 25 mM EDTA and 0.2 M citric acid adjusted to pH 7 by addition of KOH and autoclaved.

All autoclave sterilizations took place at 121 ºC for 30 minutes, except for the GPY medium, which was sterilized at 115 ºC for 15 minutes.

2.3. Encapsulation of microorganisms

A single colony of each microorganism was transferred into 5 mL LB or GPY in a sterile 50 mL Falcon® tube (Corning) and incubated at 30 °C and 200 rpm for 9 h. These cultures were used as inoculum at 1% (v/v) of 5 mL M9 medium in a sterile 50 mL Falcon tube and incubated overnight at the same conditions. After that, cells were pelleted at 9000 g for 5 min and resuspended in fresh M9 to OD_{600} 2. A 2 % (w/v) sodium alginate solution was prepared in 10 mM Tris pH 8.5 and filter sterilized. The microbial suspension was thoroughly mixed with 2% (w/v) sodium alginate

in a 1:3 volume ratio (0.25 and 0.75 mL, respectively) in a sterile Eppendorf tube. Next, hydrogel beads (HB) containing the microbial strain were obtained by an extrusion-dripping method. The mixture was drawn into a 1 mL sterile syringe (Henke-Ject) and dropwise dropped into 100 mL of 0.1 M $CaCl_2$ solution using a sterile 30GA-blunt end needle (RS Components, U.K.) from a height of 1 cm. HB were crosslinked for 30 min under magnetic agitation at 220 rpm, collected with a sterile cell strainer (VWR, USA), washed with fresh sterile $CaCl_2$ solution, and incubated for 1 min in KRH buffer. In this way we obtained the microbe-loaded HB cores used for subsequent experiments.

The layer-by-layer (LbL) coating technique was employed to sequentially add layers of coating polymers onto the HB core, resulting in HB with varying number of coating layers. Three different polymers were tested as coating agents: low MW chitosan, poly-α-L-lysine hydrochloride (αPLL, MW 15000−30000 Da) and poly-ε-L-lysine hydrochloride (εPLL, MW 3500-4500 Da).

To this end, HB cores were transferred to a 15 mL Falcon tube containing 5 mL of 1 mg/mL solution of polylysine (either εPLL or αPLL) on KRH buffer, incubated for 10 min under gentle agitation and washed with fresh KRH buffer. The HB were added straightaway to 80 mL of 0.2 % (w/v) alginate solution in 10 mM Tris pH 8.5 and kept under magnetic stirring at 220 rpm for 10 min. Next, the HB were rinsed and incubated with KRH buffer, and incubated again with εPLL/αPLL-KRH solution for 10 min. The HB were then washed with 0.15 M sterile mannitol, transferred to 5 mL of 1 mg/mL solution of εPLL/αPLL in 0.15 M mannitol and incubated for 2 h. The resulting beads will be referred onwards as three-layers εPLL hydrogel beads or αPLL hydrogel beads (3L-εPLL-HB or 3L-αPLL-HB respectively). Finally, HB with an additional outer layer of alginate were also produced. For that, the 3L HB were rinsed with KRH buffer and incubated in the 0.2% (w/v) alginate solution for 10 min, washed with KRH buffer and submerged in a crosslinking solution with 50 mM $BaCl_2$ and 0.15 M mannitol for 5 min under magnetic agitation at 220 rpm. Consequently, these HB will be referred as four-layers HB **(**4L-εPLL-HB or 4L-αPLL-HB). After the addition of the last coating layer, HB were rinsed and maintained in PBS buffer. The protocol described was modified when chitosan was used as coating polymer, as detailed in the supplementary material.

2.4. Encapsulation effectiveness and microbial viability and growth

Microbe-loaded HB were incubated in culture media to evaluate microbial survival and encapsulation effectiveness. A single HB was placed in a well of a 48-well plate (Costar®) containing 0.5 mL of M9, LB or GPY medium. The HB was incubated at 30 ºC and 150 rpm for 48 h. Viability was assessed by crushing the HB and plating the contents on agar plates. The effectiveness of the encapsulation was evaluated by the detection of the presence of the encapsulated microorganism in the liquid culture medium, by plating the media on agar plates. The absence of colonies in the liquid culture was considered as effective encapsulation. HB prepared with chitosan, α-PLL, ε-PLL as coating agents and with 3 and 4 layers were tested. Wells without HB served as controls, and each condition was replicated at least eight times.

We also evaluated the growth of the encapsulated microorganisms inside the HB. For that, after 24 and 48 h of incubation, the HB was transferred to a sterile Eppendorf tube containing 1 mL of disruption buffer and vortexed for 10 minutes to dissolve the coatings of the capsules, facilitating cell release into the buffer. Colony forming units (CFUs) were then determined by plating serial dilutions of the cell suspensions on LB or GPY agar plates for bacteria and yeast respectively.

2.5. HB microscopy characterization

HB have been characterized with light and electron microscopy. HB shape, size and microbial distribution were examined using an Olympus CKX53 inverted microscope at 4x, 10x and 20x magnification. Methylene blue-stained and unstained HB were visualized immediately after preparation and after incubation in M9, LB or GPY media for 48 h. Methylene blue-stained HB were prepared by mixing HB with a 1% methylene blue solution for 1-2 minutes under gentle agitation. The HB was then washed twice with distilled water.

Prior to SEM microscopy, HB were fixed in 2.5% glutaraldehyde prepared in 0.05 M sodium cacodylate buffer for 24 h at 4 °C. Following fixation, samples were washed with 0.1 M sodium cacodylate buffer. Post-fixation was performed with 1% osmium tetroxide for 1 h at room temperature. Samples were then dehydrated through a graded ethanol series, reaching 100% ethanol, and subsequently subjected to critical point drying with CO_2 using a Leica EM CPD300 critical point dryer. Finally, HB were cut in half with a razor blade and coated with carbon using an Emitech K975X coater. After processing, HB morphology was examined using a high-resolution field emission scanning electron microscope AURIGA (Carl Zeiss SNT) equipped with an AZtec detector (Oxford Instruments).

2.6. HB storage

Fresh 3L-εPLL-HB containing *B. subtilis* were incubated for 1h in storage solution, consisting of M9 medium supplemented with 5 % (w/v) mannitol under stirring and at room temperature. HB were aliquoted and stored in the same solution. Refrigerated storage at 4 ºC and frozen storage at -80 ºC were tested. To assess the performance of the stored HB, encapsulation effectiveness and microbial viability and growth were evaluated as described above.

2.7. Spatially distributed co-cultures using HB.

Spatially distributed co-cultures (SDCC) combining encapsulated *P. putida* inside 3L-εPLL-HB and planktonic *K. marxianus* cells were performed. These consisted of 20 HB in 100 mL Erlenmeyer flasks containing 10 mL of M9-LB medium (90 % (v/v) M9 + 10 % (v/v) LB), inoculated with 3.67×10^5 yeast CFUs. In this way, the planktonic cells seed density was equivalent to the CFUs inside of the 20 just-prepared *P. putida* 3L εPLL-HB. Flasks were incubated at 30 ºC and 250 rpm for 24 h. The growth of both microbes in the SDCC was compared to co-cultures with both strains in suspension and their respective monocultures in the same conditions. Microbial growth was determined by plate counting. *P. putida* cell count was performed on LB plates supplemented with 20 µg/mL of natamycin and *K. marxianus* on LB plates supplemented with 50 µg/mL of kanamycin. All cultures were conducted in duplicate.

2.8. Toxicity tests

Tolerance and ability to grow in lignocellulosic byproducts were evaluated culturing planktonic and encapsulated cells in M9c. For that, suspension cultures at different seed density were compared to cultures of the same HB-encapsulated microbe varying the number of HB in the well (from one to five). All cultures were performed in 48-well plates and incubated in a CLARIOstar Plus Microplate Reader (BMG LABTECH) at 30 ºC and 200 rpm for 48 h. OD_{600} of suspension cultures was read every 20 min. After incubation, cell viability and encapsulation efficiency were evaluated as explained above.

3. Results

3.1. Optimization of microbial encapsulation protocol

The first requirement of the encapsulation method that we aim to develop is to ensure complete microbial containment. Therefore, we decided to optimize the coating agent used to build core-shell alginate hydrogel beads (HB). We first encapsulated several microbial strains in alginate hydrogel using an extrusion-dripping method. After the gelification of the alginate microbe-loaded spheres, we applied a Layer-by-Layer (LbL) coating technique to add successive intercalate layers of coating polymers (chitosan, αPLL or εPLL) and alginate (Fig. 1).

We evaluated the encapsulation effectiveness by incubating the HB in M9 medium for 48 hours, the results are summarized in Table 1. Three layered chitosan HB (3L-chi-HB) failed to contain all the microorganisms; however, the additional alginate layer of 4L-chi-HB ensured the containment of *B. subtilis* and *K. marxianus* (Table 1). αPLL-HB successfully encapsulated *B. subtilis* and *K. marxianus*, regardless of the coating layers in the HB. Conversely *P. putida* escaped from both 3L- and 4L-αPLL-HB, and *Y. lipolytica* remained inside of the αPLL-HB during the first 24 h of incubation, but escaped from them after 48 h. In contrast, εPLL-HB successfully encapsulated both bacterial and yeasts strains, with either 3L or 4L of coating. Next, HB that successfully contained all microorganisms in M9 medium were cultured in rich media, LB or GPY for bacteria and yeast respectively (supplementary Table 2). Under these conditions, *B. subtilis* and *K. marxianus* encapsulated in 4L-chi-HB escaped from the beads, which showed a damaged structural integrity. In the case of 3L- and 4L-αPL-HB encapsulating *B. subtilis* we did not detect structural damage, but regardless that cells escaped to the liquid medium after 48 hours of incubation of the beads. Remarkably, εPLL-HB retained their ability to contain the four microbes when incubated in rich media during this period.

In addition to the evaluation of the cell containment, we quickly assessed the microbial viability after the encapsulation and incubation. For that, we mechanically disrupted and spread over agar plates the HB. All four strains remained viable as indicated by their growth in the plates, regardless of the coating polymer and the number of coating layers (data not shown).

Considering all these observations, we selected εPLL-HB as the best performing coating agent for the preparation of core-shell alginate hydrogel beads, and focused on their further characterization and applications.

Table 1. Evaluation of the encapsulation efficacy of each microbial strain in chitosan, αPLL, and εPLL-HB with three (3L) or four (4L) coating layers. HB were cultured in M9 medium for at least 48 h in individual wells.

		Strain			
Coating polymer	Number of layers	***B. subtilis***	***P. putida***	***K. marxianus***	***Y. lipolytica***
Chitosan	3L	Escape	Escape	Escape	Escape
	4L	Containment	Escape	Containment	Escape
αPLL	3L	Containment	Escape	Containment	Escape
	4L	Containment	Escape	Containment	Escape
εPLL	3L	Containment	Containment	Containment	Containment
	4L	Containment	Containment	Containment	Containment

3.2. Microbial growth inside εPLL-HB

To assess whether HB can sustain microbial growth, we encapsulated the four microbial strains in εPLL-HB and cultured in M9 and rich medium (LB and GPY for bacteria and yest respectively). We initially observed their shape, size, and microscopic structure. Empty εPLL-HB with three and four coating layers displayed a spherical shape after their preparation, with an alginate core diameter of 1.944 ± 0.024 mm, which increased up to 1.963 ± 0.035 mm and 1.965 ± 0.031 mm with the addition of three and four coating layers, respectively (supplementary material, Table S3).

Next, we analysed the distribution of the cell colonies within the HB by optical microscopy. As showed in Figure 2.a, the distribution varied depending on the encapsulated strain, the culture medium, and the number of coating layers. In M9 medium, bacterial and yeast strains in 3L-εPLL-HB spread throughout most of the alginate core. In these images, the coating layers showed lighter than the core (particularly after 24 h of incubation), suggesting that the microbes are not proliferating in them. These initial observations however are not conclusive on whether the encapsulated microbes are escaping the HB core, and therefore we recurred to optical microscopy of stained HB and electron microscopy, as detailed in the next section. The addition of an extra coating layer led to the formation of dense colonies aggregates of *B. subtilis* and *P. putida*, concentrated in the central region of the alginate core. Similarly, *Y. lipolytica* exhibited greater density in the central region but it was also distributed towards the limits of the HB. In contrast, *K. marxianus* displayed a uniformed growth pattern in 4L-εPLL-HB. In rich media, bacterial strains in 3L-εPLL-HB showed a growth pattern like that observed in M9. However, in 4L-εPLL-HB, *B. subtilis* formed large colonies that extended across alginate, while *P. putida* displayed a distinct aggregate morphology, with small colonies spreading throughout the entire alginate core with a higher density in the central region. In contrast, when culturing encapsulated yeasts in GPY medium, HB became completely turbid.

To corroborate these observations, we analysed the cell density of the encapsulated microorganisms. For that, we disrupted the HB after 0, 24 and 48 hours of incubation and determined the CFU/mL (referred to HB volume). As shown in Figure 2.b, all strains were able to proliferate within εPLL-HB, showing a considerable increase in their CFU after 24 h of incubation on either M9 or rich medium. Notably, cell counts were higher in εPLL-HB with three coating layers compared to four layers. This could be due to the antimicrobial activity of the crosslinking agent $BaCl_2$ against bacterial strains (Figure S.2) and to the lower diffusion rate of nutrients as an additional layer is added to the HB. As expected, CFU/mL of HB cultured in rich media were higher than those incubated in minimal medium for the four strains, and in many cases reaching densities more than one order of magnitude higher. This also support the observations of the optical microscopy showed in Figure 2.a. We then compared the cell density inside the HB with that in liquid cultures in Erlenmeyer flasks with rich medium (horizontal red lines in Fig. 2b). Our initial hypothesis was that microorganisms will grow to lower cell densities when encapsulated inside HB. Indeed, this was the case for *P. putida* and *Y. lipolytica*. However, we found that *B. subtilis* reached similar cellular density inside 3L-εPLL-HB after 24 hours and inside 4L-εPLL-HB after 48 hours of incubation than the one that reached growing in suspension. Finally, *K. marxianus* showed a markedly distinct behaviour to the rest of the encapsulated strains, since it reached remarkably high cell densities when encapsulated in both 3L- and 4L-εPLL-HB, which were almost an order of magnitude higher compared to its planktonic cell density. This observation refutes our initial hypothesis and suggests that the behaviour of encapsulated microorganisms can significantly vary between different strains.

3.3. εPLL-HB characterization

To analyse the distribution and growth patterns of encapsulated microorganisms in more detail, we examined stained εPLL-HB under optical inverted microscopy at 10x and 20x magnification (Fig. 3 and Fig. S.3). As mentioned above, we observed a distinct growth pattern depending on the microbe cultured, the number of coating layers in the HB and the culture medium. Using higher magnification, we identified individual cells in just-prepared HB (0 h) located in both the core and the coating layers for the four strains tested. However, these isolated cells did not proliferate into microbial colonies as those initially placed in the alginate core did.

For bacterial strains encapsulated in 3L-εPLL-HB and incubated in M9 medium grew distributed along all the alginate core, although a higher colony density formed in the central regions. The addition of a fourth coating layer led to the formation of large bacterial colonies concentrated in the central region of the HB core, with distinctive morphologies for each strain. When 3L-εPLL-HB were cultured in rich medium, *P. putida* colonies exhibited a flattened spheroid-like morphology similar to that observed in M9 medium. In this case, colony aggregates protruded in some regions of the coating layers, and they were more dense, in agreement with the CFU counts described above. In contrast, *B. subtilis* colonies did not organise into aggregates. Colonies in 4L-εPLL-HB where higher in size compared to 3L ones when incubated in rich medium for both strains, and in this case no inclusions in the coating layer were observed.

Focussing on the encapsulated yeast, cells were also identified within the coating layers of both 3L- and 4L-εPLL-HB incubated in M9, and again these did not develop into colonies. In rich medium, the εPLL-HB containing *K. marxianus* became mostly opaque after 48 h of incubation in both 3L- and 4L-εPLL-HB, limiting further observations. This is in agreement with the high cell density that we found for yeast growing inside εPLL-HB. In contrast, *Y. lipolytica* cells remained visible within the alginate core of both 3L and 4L-εPLL-HB. It is worth mentioning that encapsulated yeast exhibited distinct morphologies. While *K. marxianus* mainly grew in yeast form, except in 4L- εPLL-HB incubated in rich medium for 24 h (picture not shown), *Y. lipolytica* we observed yeast, pseudohyphae and hyphae, combined inside each of the HB.

Next, we analysed εPLL-HB using scanning electron microscopy (SEM). Cross-sectional images allowed us to clearly distinguish the core from the coating layers in both control 3L and 4L- εPLL-HB with no cells inside (Fig. 4, Fig. S.4 and Fig. S.5). We observed significant structural differences depending on the number of coating layers. In 3L-εPLL-HB, the coating layers appeared separated from each other. In contrast, 4L-εPLL-HB exhibited a thicker and more compact alginate hydrogel core. As expected, the external structure of the HB varied depending on the outermost coating polymer. In 3L-εPLL-HB the outer surface is εPLL and appeared smooth, whereas the addition of an alginate layer in 4L-εPLL-HB resulted in a rougher texture (Fig. S.5).

SEM images of microbe-loaded εPLL-HB (Fig. 4 and Fig. S.4) illustrate that the external structure was preserved, both in 3L and 4L configurations and after 48 hours of incubation in M9 medium. While cells could be observed in contact with the inner region of the coating layer, no cells were detected in the outer side of the capsules. Interestingly, we found that central region of 3L-εPLL-HB appeared almost empty as a consequence of microbial growth. On the other hand, the structure of the alginate core remained mostly unaltered for the 4L-εPLL-HB, and groups of microbial cells are detected confined in specific regions of the alginate core, resembling the colonies observed in optical microscopy images.

3.4. Applications of the εPLL-HB

3.4.1. Spatially organised co-cultures

Following their characterization, we evaluated the applicability of εPLL-HB. For that, we employed them for the construction of a spatially organized co-culture (SOCC) of two microbial strains, wherein one of them grew in suspension and the other encapsulated within a 3L εPLL-HB. For this purpose, we selected two strains with notable differences in growth rate and cell density at their stationary phase: *P. putida* and *K. marxianus*. When cultured in suspension in M9-LB medium, *P. putida* exhibited a lag phase of approximately 2 hours and reached a cell density of 2.68×10^9 CFU/mL. In contrast, *K. marxianus* had a longer lag phase of around 6 hours and reached a density of 5.18×10^7 CFU/mL (Fig 5.a.i), nearly two orders of magnitude lower than *P. putida*. When a co-culture was established with both strains growing in suspension at equal initial densities (3.67×10^4 CFU/mL), *P. putida* reached a cell density comparable to its monoculture after 24 hours, whereas *K. marxianus* experienced a drastic 50-fold reduction in CFU/mL (Fig 5.a.ii). Conversely, when co-cultured as a SOCC, where *K. marxianus* grew in suspension and *P. putida* encapsulated within 3L εPLL-HB, the former reached the same density than its monoculture, and the latter grew inside the εPLL-HB to the same density than a control culture without *K. marxianus* in the liquid medium (Fig 5.a.iii and iv), regardless the presence of *K. marxianus* in the liquid medium.

3.4.2. Long-term preservation

We next tested the possibility to preserve 3L-εPLL-HB under two conditions: refrigerated at 4 ºC and frozen at -80 ºC. We assessed the performance of 3L-εPLL-HB on retaining their ability to avoid any cell leakage while sustaining microbial growth and evaluated the viability of the encapsulated microorganism. To do so, we quantified the viable *B. subtilis* cells within 3L-εPLL-HB after their recovery from the preservation conditions. Additionally, we incubated the 3L-εPLL-HB in M9 medium for 24 hours and analysed the microbial growth inside of them, as well as the culture medium to detect any cell escaped from the beads during the incubation (Fig 5.b).

The results reveal a big disparity between the two preservation conditions tested. At 4 ºC, the cells inside 3L-εPLL-HB rapidly died, with a 10-fold decrease in viability after 2 days of preservation compared to freshly beads, and no detectable CFUs after 7 days. In contrast, 3L-εPLL-HB frozen at -80 ºC maintained the same viable cells than the just-prepared ones for at least 64 days, without any decrease trend detected during that time. Preserved 3L-εPLL-HB incubated in M9 showed the same behaviour. Accordingly, *B. subtilis* reached the same cell density inside 3L-εPLL-HB after their incubation, regardless the duration of their storage at -80 ºC. Notably, none of the 3L-εPLL-HB tested showed any cell escape after their storage and posterior incubation in M9 medium.

3.4.3. Protection against environmental stressors

We tested the four strains growing in suspension and inside 3L-εPLL-HB in M9-coffe (M9c) medium to explore the protective properties of the hydrogel beads against the toxic and inhibitory compounds present in this lignocellulose-derived medium, which was produced through and hydrothermal hydrolysis pretreatment [24,25]. Fig5.c shows the influence of the seeding density over the growth kinetics for the four strain growing in suspension. These seeding densities where fixed to explore the concentration in the medium equivalent to the microbial content inside their respective εPLL-HB after their preparation. The results varied between

different strains. While *P. putida* seems to have a high susceptibility to the inhibitory and toxic effect of M9c and only showed a detectable OD increase when the seeding density was 10^7 CFU/mL, *B. subtilis* performed better in this medium and grew for all the densities tested, albeit the lag phase was considerably extended when decreasing the seeding density. Both of the yeast performed similarly and only showed a significant growth with the two highest inoculum cell densities. Complementarily to the OD measurements, we took samples of all these cultures and plated a 20 µL drop in LB/GPY-agar in order to detect viable cells. None of the *P. putida* cultures had viable cells with the exception of the one that showed growth in the plate reader, which confirms that besides not growing the bacteria died in all the cultures were an OD increase was not detected. Accordingly, viable cells were found in all the *B. subtilis* cultures. Interestingly, for both of the yeasts, we also found viable CFU in those cultures where no OD increase was detected. Since the CFU found increased in number with their correspondent inoculum cell density, this observation suggests a sporulation induced by the M9c and that the yeast did not replicate until they were seeded at a critical inoculum cell density.

Next, we performed a similar experiment with the microbes encapsulated inside εPLL-HB. For that, we ran other seeding density screening adding between 1 and 5 εPLL-HB to 0.5 mL of M9c (equivalent seeding densities are detailed in supplementary table 4). At the end of the culture the beads were mechanically disrupted and their whole content plated on LB/GPY-agar. All the εPLL-HB kept viable CFU after their incubation on M9c. Interestingly, the cell density of the spread HB was similar, irrespective of the number of beads used, for all the strains except for *Y. lipolytica*. In the case of the latter, the number of viable CFU increased for experiments using one bead to those with four.

4. Discussion

4.1. Optimization of coating agent

The main purpose of this work is to design a microbial encapsulation method that ensures complete microbial containment while allowing the encapsulated cells to proliferate and reach cell densities comparable to those they will reach in suspension cultures. To achieve that, the encapsulating material must be chemically and mechanically resistant to maintain its structural integrity and prevent cell escape during the culture. But at the same time the material should be flexible to allocate the new cells as they multiply and allow their chemical interaction with the liquid medium to get access to the nutrients required for their basal metabolism and replication. Taking all of this in consideration, we selected alginate-based core-shell encapsulation as a promising approach.

We initially tested the performance of three coating agents. Two of them, chitosan and αPLL are polymers commonly used to prepare core-shell alginate hydrogel beads. The third one, εPLL, has been barely explored to that end. In fact, to our knowledge, only Ma et al. et al reported the use of this polymer to prepare alginate capsules containing CHO cells [26].

A preliminary antimicrobial assay of the coating polymers showed that, of the three coating polymers, only chitosan did not inhibit microbial growth (Figure S.1). On the other hand, αPLL and εPLL, which are commonly used as antimicrobial agents [27–29], inhibited the growth to varying degrees depending on the strain, except for *Y. lipolytica*, which was unaffected by both of them. However, when considering the use of these polymers as coating agents, εPLL clearly performed better than the other two. Regarding the structural integrity of the HB, both poly

lysines formed stable HB that maintained their structural integrity after their incubation in minimal medium, but chitosan HB (chi-HB) only were stable when prepared with four coating layers. We also observed some adhesion between chi-HB just after their preparation, which can significantly hinder their applicability and compromise their encapsulation efficacy. Concerning the efficacy of the microbial containment inside the HB, we detected clear advantages of εPLL compared to αPLL: while no escape was detected from εPLL-HB, *P. putida* and *Y. lipolytica* escaped from αPLL-HB. Interestingly, *P. putida* is the smallest strain tested and *Y. lipolytica* was found to grow as pseudohyphae and hyphae inside HB. Either cell size and morphology can challenge the complete containment inside the beads, and in both cases εPLL demonstrated to contain both microorganisms inside the HB.

Chemical stability is another crucial feature for alginate beads. Under our experience non-coated alginate beads quickly lost their structural integrity when incubated in standard complex media such as LB and GPY (using for example a few hundreds of µL of culture medium to incubate one bead of around 4 µL in a well plate), which justifies the need of a coating agent. In our experiments chi-HB performed also poorly in these complex media. HB prepared with both for the lysine polymers retained their structural integrity. However, while αPLL-HB failed on avoiding the release of the microorganisms that did not escaped from them in M9 medium εPLL-HB were equally effective and no microbial scape from them was detected. Finally, swelling has been previously observed for beads formed only with alginate or these coated with chitosan during their incubation [16,18]. However, εPLL-HB did not show a significant swelling after their incubation (Table S.6). This observation also pinpoints the mechanical resistance of this coating agent, and the consequent prevention of the formation of cracks on the HB that will compromise its encapsulation efficacy. Summarizing, εPLL showed a superior microbial encapsulation efficacy and preservation of the structural integrity alginate core. In addition, its price is orders of magnitude lower than αPLL, since it is naturally produced while αPLL is a synthetic polymer [26]. Therefore, we consider that εPLL is a promising coating agent for the preparation of core-shell alginate hydrogel beads, that outperformed other two coatings commonly used by many cell encapsulation protocols.

4.2. Microbial growth inside εPLL-HB

Once εPLL was identified as the best performing coating agent, we evaluated its compatibility with the growth of several encapsulated microbes. The four tested strains multiplied by a factor of one to three orders of magnitude when cultured inside εPLL-HB, which demonstrates the compatibility of this polymer with microbial growth in the alginate hydrogel core of the bead. In most cases, cell density inside the HB depended more on the number of coating layers than the culture medium used. We identify two factors that can contribute to that, the lower mass transfer in 4L-HB and the microbial toxicity effect of the $BaCl_2$ used to crosslink the outer alginate coating layer of 4L-HB (Figure S2). This creates a trade-off between cell density and resistance of the capsule, that can be adjusted depending on the desired application. Curiously, *K. marxianus* reached considerably a higher cell density encapsulated inside 3L-εPLL-HB than growing in suspension. This could be influenced by the higher resource availability since the microbial growth is restricted to the interior of the bead. But despite of that, the high cell density reached could be of interest for applications in bioreactors, since it will allow to achieve higher cell densities in the system or to reduce working volumes while maintaining the same microbial load.

Microscopy observations of the εPLL-HB revealed different cellular and colony morphologies depending on the species, number of coating layers and culture medium. SEM images also revealed that the internal alginate 3D structure was considerably altered as a result of the microbial growth, as evidenced by the big internal cavities observed on 3L-εPLL-HB and their smaller size on 4L ones. Despite variability on the observed bead, colony and cell morphology for each of the species and condition tested, no damage of the external coating layers was detected in any of the εPLL-HB after incubation either. This confirms that alginate core-shell beads prepared with εPLL are versatile and reliable, and that could be used to encapsulate a wide variety of microorganisms with varied their size or growing morphology.

4.3. Applications of εPLL-HB

Regarding the potential uses of the εPLL-HB, this study successfully demonstrated that alginate core-shell HB preparations based on εPLL effectively are a useful tool for constructing spatially organized microbial co-cultures (SOCC). 3L-εPLL-HB exhibited excellent reliability, since they endured the mechanical stress of the vigorous shaking of 250 rpm used during the SOCC experiments and avoided the escape of the entrapped *P. putida*, the most challenging to encapsulate strain tested in this work due to its small size. Despite the εPLL moderate antimicrobial activity observed in well diffusion assays (Fig S.1), planktonic *K. marxianus* growth in the SOCC was unaffected by its contact with the 3L-εPLL-HB, suggesting that the polymer's antimicrobial effect marginal in this co-culture configuration. Indeed, *K. marxianus* growing in suspension reached the same cell densities in both the SOCC and the monoculture control (Fig 4.a), which proves that microbial species with a high disparity on their growth rates can be co-cultured using this system. In addition, we plated the liquid medium on natamycin LB-agar to assess bacterial escape from the 3L-εPLL-HB. Each experiment utilized twenty 3L-εPLL-HB in 10 mL of culture and remarkably, no bacterial colonies were detected in either in the SOCC or the control experiment. This confirms the robustness and reproducibility of the co-cultures based on εPLL-HB and highlights the potential application to scale-up synthetic microbial consortia. Furthermore, SOCC built based on εPLL-HB offer precise control over microbial population distribution. In this study, we used a ratio of 2 HB per mL of liquid culture, but this could be readily adjusted to achieve the desired relative abundances of the species within the co-culture. Thus, the successful encapsulation of all tested strains points out the broad applicability of this approach to various combinations of planktonic and encapsulated microorganisms.

Although 4L-εPLL-HB were not evaluated in SOCC, these could be used to build SOCCs using other media, such as LB, that have demonstrated higher disruptive activity against alginate hydrogels, since the additional coating alginate layer on improved their chemical resistance. Therefore, 4L-εPLL-HB could expand SOCC applicability to mediums where otherwise this cell encapsulation approach will not be applicable or show a lower efficacy. Besides, in addition to improving the mechanical properties of the εPLL-HB, the outer alginate layer can potentially mitigate the antimicrobial effects of εPLL on microorganisms more susceptible to it than *K. marxianus*.

The compatibility with long-tern preservation of alginate core-shell beads is crucial for their applicability. The possibility to storage ready-to-use HB will significantly contribute to optimize the manufacturing and set-up work required, as well as as increase the batch-to-batch reproducibility. Therefore, we explored the performance of 3L-εPLL-HB refrigerated at 4 ºC and frozen at -80 ºC. We paid particular attention to whether the beads remained effective on

isolating all the encapsulated and growing cells from the liquid surroundings, or otherwise the freezing step disrupted the coating layers to and extend that cells would be released. Also, for both preservation conditions, we determined cell viability of inside the preserved 3L-εPLL-HB and to what extent they sustained cell growth when incubated.

The physical integrity of the coating layer, evaluated as its ability to avoid cell escape, remained unaltered for both preservation methods. However, regarding the cell viability, it quickly was reduced to zero for refrigerated 3L-εPLL-HB. We observed that the beads shrunk during the refrigeration, which suggest that cell death could be the result of an osmolar unbalance between the HB and the storage buffer. On the other hand, *B. subtilis* viability and their ability to proliferate inside 3L-εPLL-HB frozen at -80ºC remained unchanged for at least 64 days of storage. To our knowledge, this is the first report on alginate core-shell beads encapsulating a bacterium that can be frozen while retain their properties unaltered. This also represent a promising result to optimize the εPLL-HB storage conditions at more moderate temperatures.

The third 3L-εPLL-HB feature evaluated was their ability to protect cells against environmental stressors. Many lignocellulose-derived substrates are rich in phenolic compounds or furfurals which are produced during their pretreatments. These are toxic for some microorganisms and therefore hinder the valorisation of these subproducts through biotechnological processes. The encapsulation inside 3L-εPLL-HB proved to be protective against the toxic effects that the M9c medium for *P. putida*, which did not grow in suspension at seeding densities equal or lower than 5×10^6 CFU/mL. On the other hand, viable *P. putida* strains were found inside 3L-εPLL-HB after their incubation on this medium, at remarkably lower initial cell densities (from 3.74×10^4 to 1.78×10^5 CFU/ml, for 1 and 5 3L-εPLL-HB per well respectively). Besides, all of the HB showed similar cell densities, which suggest that the bacteria proliferated inside of them irrespective of the number of 3L-εPLL-HB present in the well.

Two protective factors could be in play here. First, the higher local cell densities inside the HB could help to maintain a critical mass of viable cells that can deal with these stressors substances and degrade them. However, the M9c medium was toxic for *P. putida* growing in suspension at seeding densities up to 5×10^6 CFU/mL and even at 10^7 CFU/mL the lag phase extended for almost 20 h. On the other hand, the local cell density inside the beads is 4.5×10^6 CFU/mL ± 1.14×10^6 CFU/mL. This suggest there are more effects in play that protects this bacterium against toxic compounds other than the cell density in the local environment of the HB. More specifically, the limitations to the mass transfer to the inside of the bead could play a beneficial role in this case, leading to a lower concentration in the interior than in the liquid medium, which in turn would reduce the stress over the cells and even facilitate their gradual metabolization.

5. Conclusions

In this work, we have identified the need for a systematic evaluation and optimization of microbial encapsulation that ensures a complete microbial containment and enables a significant microbial proliferation.

Here, we introduce an optimized method for microbial encapsulation using alginate-based core-shell hydrogel beads (HB) with ε-poly-L-lysine (εPLL) as the coating agent. HB prepared with εPLL demonstrated superior microbial containment capabilities and robustness under diverse culture conditions compared to other commonly used coatings like chitosan and α-poly-L-lysine. εPLL-HB showed to be suitable to encapsulate and allow the growth of diverse

bacteria and yeast species with diverse sizes and cellular and colony morphologies. Therefore, we consider of this method can be extended to the encapsulation of many other microbial strains and prevent them to escape from the confined spaces.

The εPLL-HB enabled successful construction of spatially organized co-cultures, effectively maintaining population balance between microorganisms with disparity in growth rates and offering protection against environmental stressors. Additionally, they exhibited excellent performance in long-term preservation at -80 ºC, without compromising structural integrity or decreasing the microbial viability and ability to grow inside of them.

Considering all these factors and the reduced price of εPLL, εPLL-HB offer a scalable and cost-effective tool for synthetic microbial consortia engineering applicable to a wide variety of microorganisms, which can unlock their application in diverse biotechnological processes.

6. Author contributions

AAC: data curation, formal analysis, investigation, methodology, writing-original draft. MGR: supervision, validation, writing-review and editing. IMR: conceptualization, funding acquisition, methodology, supervision, project administration, validation, writing-review and editing

7. Acknowledgements

The authors acknowledge funding through grant TED2021-131194 A-I00 funded by MCIN/AEI/ /10.13039/501100011033 and NextGenerationEU/PRTR. IMR also acknowledges the financial support by grant RYC2022-037570-I funded by MICIU/AEI/10.13039/501100011033 and by ESF+.

8. References

[1] A. Sanchez, D. Bajic, J. Diaz-Colunga, A. Skwara, J.C.C. Vila, S. Kuehn, The community-function landscape of microbial consortia, Cell Syst 14 (2023) 122–134. https://doi.org/10.1016/j.cels.2022.12.011.

[2] M. Zhang, F. Han, Y. Li, Z. Liu, H. Chen, Z. Li, Q. Li, W. Zhou, Nitrogen recovery by a halophilic ammonium-assimilating microbiome: A new strategy for saline wastewater treatment, Water Res 207 (2021) 117832. https://doi.org/10.1016/J.WATRES.2021.117832.

[3] C. Kost, K.R. Patil, J. Friedman, S.L. Garcia, M. Ralser, Metabolic exchanges are ubiquitous in natural microbial communities, Nat Microbiol (2023). https://doi.org/10.1038/s41564-023-01511-x.

[4] L. Lin, Bottom-up synthetic ecology study of microbial consortia to enhance lignocellulose bioconversion, Biotechnology for Biofuels and Bioproducts 15 (2022) 1–15. https://doi.org/10.1186/S13068-022-02113-1/FIGURES/4.

[5] M. Wang, X. Chen, X. Liu, Y. Fang, X. Zheng, T. Huang, Y.Q. Tang, M. Ackermann, Y. Nie, X.L. Wu, Even allocation of benefits stabilizes microbial community engaged in metabolic division of labor, Cell Rep 40 (2022). https://doi.org/10.1016/j.celrep.2022.111410.

[6] Y.Y. Liu, Controlling the human microbiome, Cell Syst 14 (2023) 135–159. https://doi.org/10.1016/j.cels.2022.12.010.

[7] S.P. Zhou, X. Ke, L.Q. Jin, Y.P. Xue, Y.G. Zheng, Sustainable management and valorization of biomass wastes using synthetic microbial consortia, Bioresour Technol 395 (2024). https://doi.org/10.1016/j.biortech.2024.130391.

[8] R.L. Shahab, S. Brethauer, M.P. Davey, A.G. Smith, S. Vignolini, J.S. Luterbacher, M.H. Studer, A heterogeneous microbial consortium producing short-chain fatty acids from lignocellulose, Science (1979) 369 (2020) eabb1214. https://doi.org/10.1126/science.abb1214.

[9] A. Millán Acosta, D. Cosovanu, P. Cabañeros López, S.T. Thomsen, K. V. Gernaey, R. Canela-Garayoa, Co-cultivation of a novel Fusarium striatum strain and a xylose consuming Saccharomyces cerevisiae yields an efficient process for simultaneous detoxification and fermentation of lignocellulosic hydrolysates, Chemical Engineering Journal 426 (2021) 131575. https://doi.org/10.1016/j.cej.2021.131575.

[10] Y. Jiang, Designing Synthetic Microbial Consortia for Biofuel Production, Trends Biotechnol 38 (2020) 825–828. https://doi.org/10.1016/j.tibtech.2020.02.010.

[11] J. Hu, Y. Xue, H. Guo, M. tian Gao, J. Li, S. Zhang, Y.F. Tsang, Design and composition of synthetic fungal-bacterial microbial consortia that improve lignocellulolytic enzyme activity, Bioresour Technol 227 (2017) 247–255. https://doi.org/10.1016/j.biortech.2016.12.058.

[12] Y. Sulbaran-Bracho, M. Orellana-Saez, J. Castro-Severyn, C. Galbán-Malagón, E. Castro-Nallar, I. Poblete-Castro, Continuous bioreactors enable high-level bioremediation of diesel-contaminated seawater at low and mesophilic temperatures using Antarctic bacterial consortia: Pollutant analysis and microbial community composition, Environmental Pollution 321 (2023). https://doi.org/10.1016/j.envpol.2023.121139.

[13] F. Senne de Oliveira Lino, D. Bajic, J.C.C. Vila, A. Sánchez, M.O.A. Sommer, Complex yeast–bacteria interactions affect the yield of industrial ethanol fermentation, Nature Communications 2021 12:1 12 (2021) 1–12. https://doi.org/10.1038/s41467-021-21844-7.

[14] Á. Sánchez, A. Arrabal, M. San Román, J. Díaz-Colunga, The optimization of microbial functions through rational environmental manipulations, Mol Microbiol (2024). https://doi.org/10.1111/mmi.15236.

[15] L. Wang, X. Zhang, C. Tang, P. Li, R. Zhu, J. Sun, Y. Zhang, H. Cui, J. Ma, X. Song, W. Zhang, X. Gao, X. Luo, L. You, Y. Chen, Z. Dai, Engineering consortia by polymeric microbial swarmbots, Nature Communications 2022 13:1 13 (2022) 1–13. https://doi.org/10.1038/s41467-022-31467-1.

[16] I. Moya-Ramírez, P. Kotidis, M. Marbiah, J. Kim, C. Kontoravdi, K. Polizzi, Polymer Encapsulation of Bacterial Biosensors Enables Coculture with Mammalian Cells, ACS Synth Biol 2022 (2022) 1303–1312. https://doi.org/10.1021/ACSSYNBIO.1C00577/SUPPL_FILE/SB1C00577_SI_001.PDF.

[17] T.G. Johnston, S.F. Yuan, J.M. Wagner, X. Yi, A. Saha, P. Smith, A. Nelson, H.S. Alper, Compartmentalized microbes and co-cultures in hydrogels for on-demand bioproduction and preservation, Nat Commun 11 (2020) 1–11. https://doi.org/10.1038/s41467-020-14371-4.

[18] Y. Jeong, J. Irudayaraj, Hierarchical encapsulation of bacteria in functional hydrogel beads for inter- and intra- species communication, Acta Biomater 158 (2023) 203–215. https://doi.org/10.1016/j.actbio.2023.01.003.

[19] G.A. Paredes Juárez, M. Spasojevic, M.M. Faas, P. de Vos, Immunological and technical considerations in application of alginate-based microencapsulation systems, Front Bioeng Biotechnol 2 (2014) 1–15. https://doi.org/10.3389/fbioe.2014.00026.

[20] K.Y. Lee, D.J. Mooney, Hydrogels for tissue engineering, Chem Rev 101 (2001) 1869–1879. https://doi.org/10.1021/CR000108X/ASSET/IMAGES/LARGE/CR000108XF00012.JPEG.

[21] G. Simó, E. Fernández-Fernández, J. Vila-Crespo, V. Ruipérez, J.M. Rodríguez-Nogales, Research progress in coating techniques of alginate gel polymer for cell encapsulation, Carbohydr Polym 170 (2017) 1–14. https://doi.org/10.1016/j.carbpol.2017.04.013.

[22] B.J. Kim, T. Park, H.C. Moon, S.Y. Park, D. Hong, E.H. Ko, J.Y. Kim, J.W. Hong, S.W. Han, Y.G. Kim, I.S. Choi, Cytoprotective alginate/polydopamine core/shell microcapsules in microbial encapsulation, Angewandte Chemie - International Edition 53 (2014) 14443–14446. https://doi.org/10.1002/anie.201408454.

[23] P. Li, M. Müller, M.W. Chang, M. Frettlöh, H. Schönherr, Encapsulation of Autoinducer Sensing Reporter Bacteria in Reinforced Alginate-Based Microbeads, ACS Appl Mater Interfaces 9 (2017) 22321–22331. https://doi.org/10.1021/acsami.7b07166.

[24] R. Wang, Z. Lin, S. Meng, S. Liu, Z. Zhao, C. Wang, Q. Yin, Effect of lignocellulosic components on the hydrothermal carbonization reaction pathway and product properties of protein, Energy 259 (2022) 125063. https://doi.org/10.1016/J.ENERGY.2022.125063.

[25] L. Lara-Ramos, A. Cervera-Mata, J. Fernández-Bayo, M. Navarro-Alarcón, G. Delgado, A. Fernández-Arteaga, Hydrochars Derived from Spent Coffee Grounds as Zn Bio-Chelates for Agronomic Biofortification, Sustainability (Switzerland) 15 (2023) 10700. https://doi.org/10.3390/SU151310700/S1.

[26] Y. Ma, Y. Zhang, Y. Liu, L. Chen, S. Li, W. Zhao, G. Sun, N. Li, Y. Wang, X. Guo, G. Lv, X. Ma, Investigation of alginate–ϵ-poly-L-lysine microcapsules for cell microencapsulation, J Biomed Mater Res A 101A (2013) 1265–1273. https://doi.org/10.1002/JBM.A.34418.

[27] R. Ye, H. Xu, C. Wan, S. Peng, L. Wang, H. Xu, Z.P. Aguilar, Y. Xiong, Z. Zeng, H. Wei, Antibacterial activity and mechanism of action of ε-poly-l-lysine, Biochem Biophys Res Commun 439 (2013) 148–153. https://doi.org/10.1016/J.BBRC.2013.08.001.

[28] E. Lebaudy, C. Guilbaud-Chéreau, B. Frisch, N.E. Vrana, P. Lavalle, The High Potential of ε-Poly-l-Lysine for the Development of Antimicrobial Biomaterials, Adv Nanobiomed Res 3 (2023) 2300080. https://doi.org/10.1002/ANBR.202300080.

[29] H. Zhu, R. Liu, Y. Shang, L. Sun, Polylysine complexes and their biomedical applications, Engineered Regeneration 4 (2023) 20–27. https://doi.org/10.1016/J.ENGREG.2022.11.001.

9. Figures

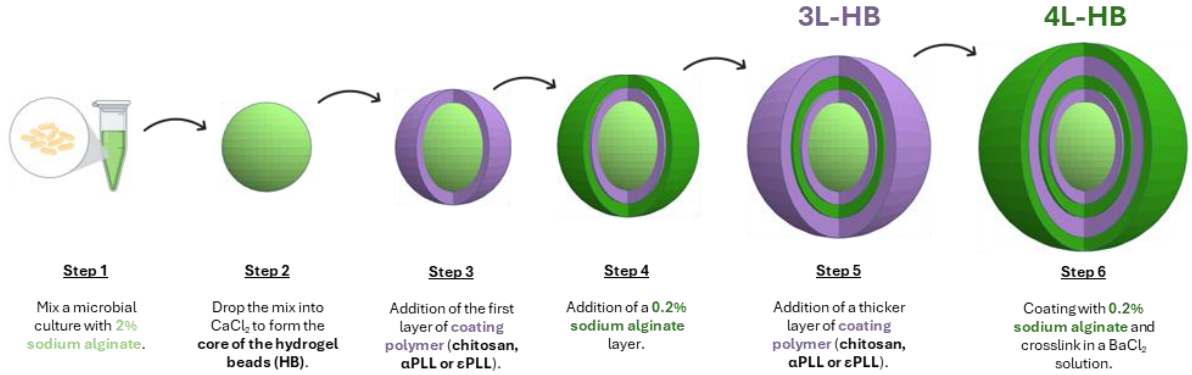

Figure 1. Schematic representation of the encapsulation method and layer-by-layer coating to obtain microbe-loaded HB with three and four coating layers.

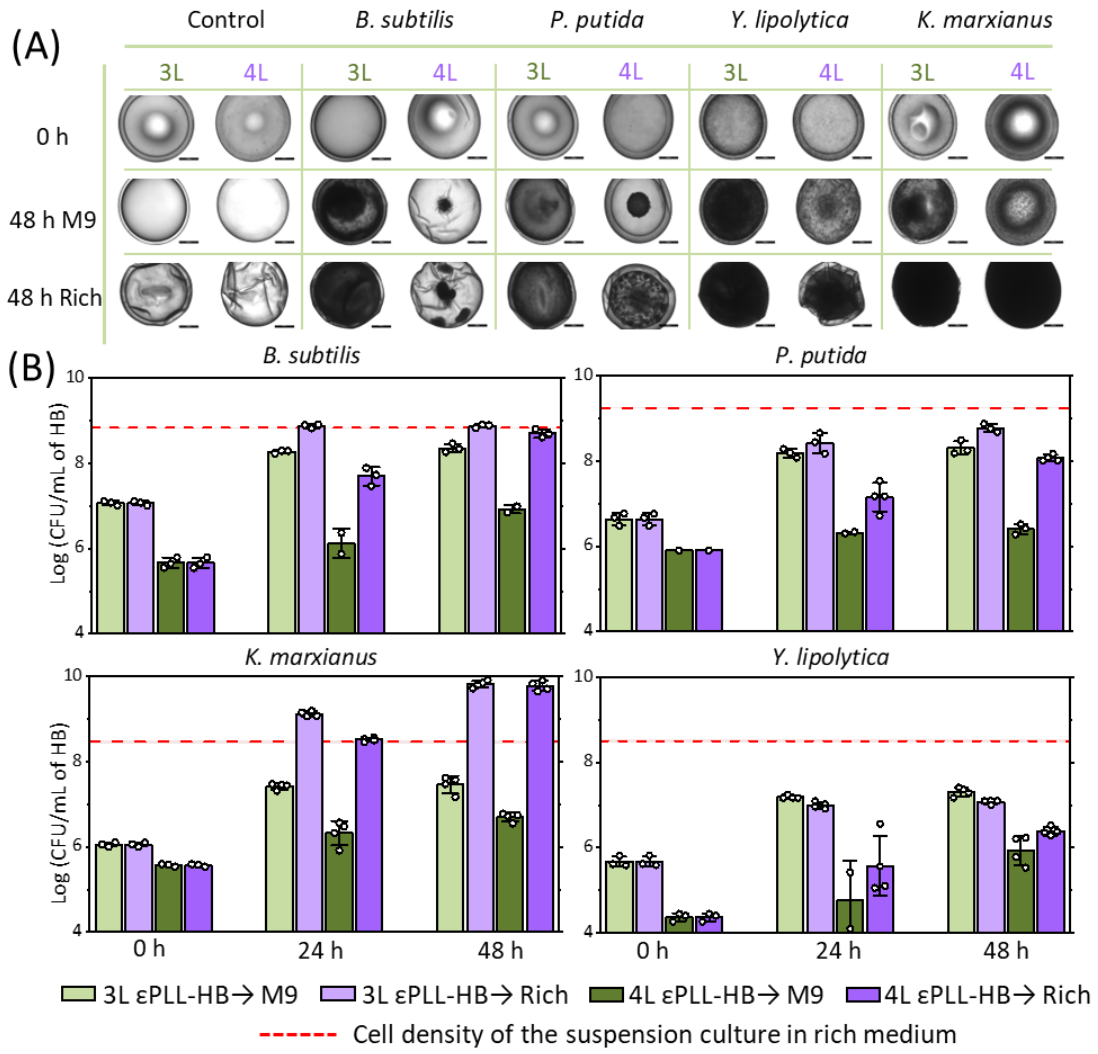

Figure 2. **(a)** Microscope images of εPLL-HB loaded with four different microbial strains, prepared with three layers (3L) and 4 layers (4L) of coating. The pictures show the just-prepared HB (0 h) and those incubated 48 h in M9 or rich medium (LB and GPY for HB containing bacteria and yeast strains respectively). Scale bar: 500 µm. **(b)** CFU per mL of HB at different incubation times and culture media (M9 and rich medium, LB and GPY for bacteria and yeast respectively). At least three independent biological replicates were run (results for each experiment indicated by circles), bars represent the average and error bars the standard deviation. The horizontal dashed red line represents the CFU/mL of the microorganism in rich medium growing in a suspension culture, and the shadowed area the SD.

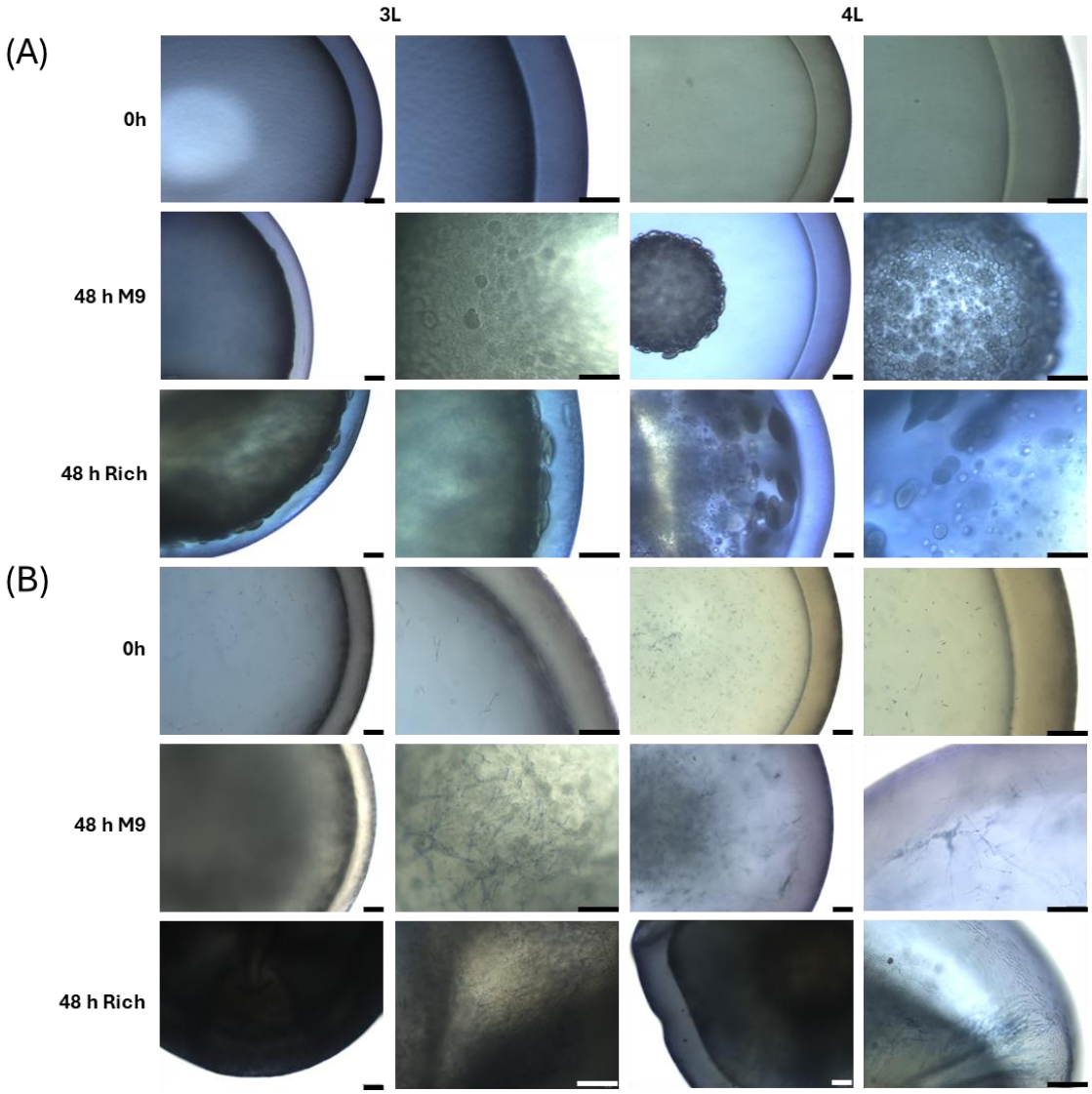

Figure 3. Optical microscope images of stained εPLL-HB with three layers (3L) and 4 layers (4L) of coating loaded with *P. putida* (A) and *Y. lipolytica* (B). The pictures show the just-prepared HB (0 h) and those incubated 48 h in M9 or rich medium (LB and GPY for HB containing bacteria and yeast strains respectively). Scale bars: 100 μm.

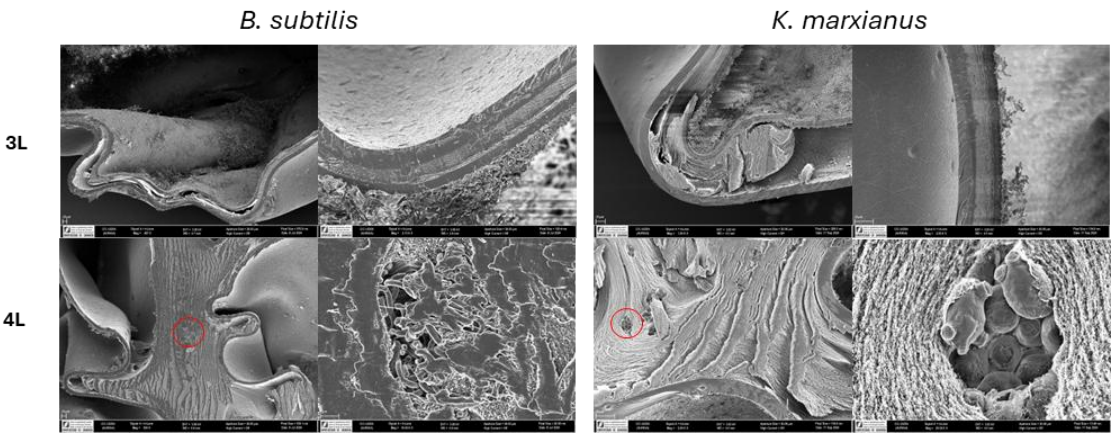

Figure 4. SEM images of stained εPLL-HB with three layers (3L) and 4 layers (4L) of coating loaded with *B. subtilis* and *K. marxianus* after their incubation for 48 h in M9 medium. Scale bars: 10 μm.

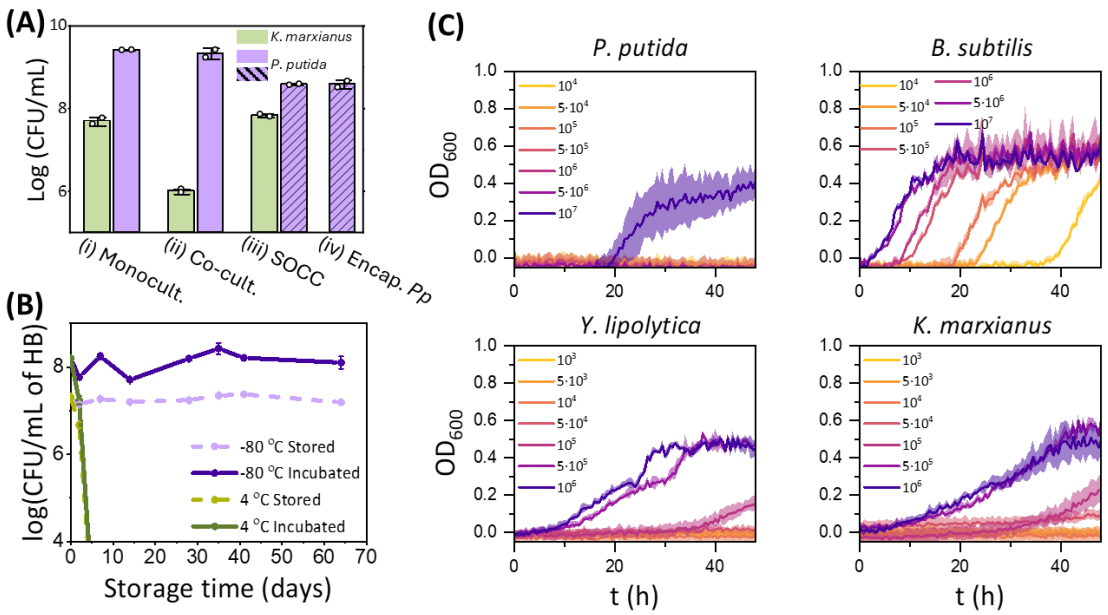

Figure 5. **(a)** (i) Cell density of *K. marxianus* and *P. putida* grown in different conditions: (i) separately in suspension monocultures; (ii) combined in a suspension co-culture; (iii) as a spatially organized co-culture with the *K. marxianus* in suspension and *P. putida* encapsulated inside 3L εPLL-HB; and (iv) a monoculture of P. putida growing inside εPLL-HB. Cell density units are expressed as log (CFU/mL), referred to the 0.5 mL of liquid medium for planktonic growing cells, and to εPLL-HB volume for encapsulated *P. putida*. Independent biological duplicates were run (results for each experiment indicated by circles), bars represent the average and error bars the standard deviation (**b**) Evolution of the cell density of *B. subtilis* encapsulated inside 3L-εPLL-HB and preserved at 4ºC and -80 ºC. Cell density was tested right after their recovery from storing conditions and adjustment to room temperature and after their incubation in M9 medium during 24 h after the specified storage time. Results correspond to the average of duplicates. **(c)** Growth kinetics (measured as optical density at 600 nm, blank subtracted using fresh M9c) of the four microbial strains in 0.5 mL of M9c medium at different seeding densities (CFU/mL). Experiments were performed by triplicate.